Solid-State Electronics 69 (2012) 67–71

Contents lists available at SciVerse ScienceDirect

Solid-State Electronics

journal homepage: www.elsevier.com/locate/sse

Red- and white-emitting organic light-emitting diodes based on trimetallic dendritic europium (III) complex: $Eu_3(DBM)_9(TMMB)$

Lili Chen [a], Binbin Wang [c], Liming Zhang [b], Dongxia Zhu [a], Peng Li [a], Zhongmin Su [a,*], Bin Li [a,b,*]

[a] Institute of Functional Material Chemistry, Faculty of Chemistry, Northeast Normal University, Changchun 130024, People's Republic of China
[b] Key Laboratory of Excited State Processes, Changchun Institute of Optics, Fine Mechanics and Physics, Chinese Academy of Sciences, Changchun 130033, People's Republic of China
[c] Changchun Normal University, Changchun 130000, People's Republic of China

ARTICLE INFO

Article history:
Received 11 July 2011
Received in revised form 27 October 2011
Accepted 4 December 2011
Available online 16 January 2012

The review of this paper was arranged by Dr. Y. Kuk

Keywords:
Europium complex
Dendritic
Electroluminescence

ABSTRACT

The photoluminescence (PL) and electroluminescence (EL) properties of a trimetallic dendritic europium (III) complex containing three metal cores as branching centers, tris(dibenzoylmethanato) (1,3,5-tris[2-(2′-pyridyl)benzimidazoly]methyl-benzene)-europium (III) ($Eu_3(DBM)_9(TMMB)$), have been investigated and reported. Red and white emissions have been acquired in the four EL devices of device A–D. Characteristic red emission peaking at 613 nm with four shoulder bands due to the $^5D_0 \rightarrow {}^7F_j$ ($j = 0$–4) transitions of $Eu_3(DBM)_9(TMMB)$ is observed in devices A–C. Device D with a simple non-doping device structure showed a white emission band. Also, the optical and the electrochemical properties of $Eu_3(DBM)_9(TMMB)$ have been characterized to possess a better understanding on the intramolecular energy transfer process. It is concluded that dendritic structure with three DBM ligands as "absorption antennas" facilitates the energy absorption and transportation of the complex.

1. Introduction

Organic dyes and polymers have been widely applied in organic light-emitting diodes (OLEDs), and further in full-color flat panel displays, because of their outstanding emissive characters. Especially, tertiary europium (III) complexes have received extensive attention as red-emitting materials for OLED owing to their sharp pure red monochromic emission and high emission quantum efficiency (up to 100%, theoretically) since the transition is not restricted by the spin inhibition rule [1]. However, the poor carrier-transporting ability, the low extinction coefficient, intense luminescence quenching by matrix vibrations like hydroxyl groups *via* non-radioactive pathways, and the low thermal stability limit their applications in OLED field [2].

Europium (III) complexes have been widely researched. $Eu(DBM)_3$bath has been used to construct the color-tuning organic light-emitting diodes controlled by voltage. Making use of Eu^{3+} featuring a sharp red emission, reversible voltage-controlled continuous color tuning is achieved in the OLEDs by using $Eu[DBM]_3$bath as the strategic starting point close to the red corner of the CIE chromaticity diagram [3]. Eu^{3+} complex is also used to mix with Tb complex to introduce another decay channel for excited Tb ions and accelerates its decay process [4].

Dendritic europium (III) complexes, as a group of third class luminescent materials for OLEDs [5,6], have several interesting properties [7–9], such as promising carrier-transporting, site isolation [10], antenna effect [11], excellent film-forming, thermal and morphological stability [12]. Many successful examples using dendritic Eu(III) complexes as emitters have been reported [10,13–15]. For example, Tian et al. synthesized a few dendritic Eu(III) complexes containing terminal frafted carbazole moieties, [Eu(MCPD)$_3$(phen)], [Eu(BCPD)$_3$(phen)] and [Eu(TCPD)$_3$(phen)]. A red emission peaking at 615 nm from $^5D_0 \rightarrow {}^7F_2$ transition of Eu(III) ion has been observed for complexes in solutions or solid films. White light emission with CIE coordinates of (0.333, 0.348) has been achieved in Eu(TCPD)$_3$(phen)-based device. The maximum external quantum efficiency is more than 1.1% and the maximum brightness is as high as 229 cd m^{-2} [10]. Two carbazole-based bipolar structural ligands, CPPO and CPO, and their corresponding Eu(III) complexes have been synthesized by Xu et al. [13]. The doping device with a configuration of ITO/NPB/1: CBP/BCP/Alq$_3$/Mg:Ag shows a maximum brightness of 1271 cd m^{-2} with external quantum efficiency of 3.6%. All devices mentioned above are based on mono-core Eu(III) complexes, and complexes with triple-core have not been investigated to the best of our knowledge.

In this work, a triple-core dendritic [15] europium complex, tris (dibenzoylmethanato) (1,3,5-tris[2-(2′-pyridyl)benzimidazoly]methyl-benzene)-europium (III), or $Eu_3(DBM)_9(TMMB)$, was synthesized

* Corresponding authors. Address: Institute of Functional Material Chemistry, Faculty of Chemistry, Northeast Normal University, Changchun 130024, People's Republic of China. Fax: +86 431 85099108 (Z. M. Su).
E-mail address: zmsu@nenu.edu.cn (Z.M. Su).

0038-1101/$ - see front matter © 2011 Elsevier Ltd. All rights reserved.
doi:10.1016/j.sse.2011.12.005

and used as the luminescent material to construct high efficiency red and white emitting OLEDs.

2. Experimental details

2.1. Preparation and characterization of $Eu_3(DBM)_9(TMMB)$

The molecular structure of $Eu_3(DBM)_9(TMMB)$ is shown in Fig. 1.

Dendritic europium complex $Eu_3(DBM)_9(TMMB)$ was synthesized as reported in Ref. [10] with some minor modifications. A mixture of mesitylene (2.8 ml, 0.02 mol), N-bromosuccinimide (10.62 g, 0.06 mol), and benzoyl peroxide (0.11 g) in CCl_4 (40 ml) was stirred and heated in N_2 at 90 °C for 12 h. After filtration, the filtrate was washed with water and dried with anhydrous Mg_2SO_4. Colorless crystals with needle structure were collected by centrifugation in the CCl_4 solution. The recrystallization with ethanol/hexance (1:1, v/v) solution afforded 6.56 g product (yield, 92%). ^1H NMR (CD_3OD): δ 4.55 (s, 6H), 7.42 (s, 3H). A mixture of 1,3,5-tris(bromomethyl) benzene (0.357 g, 1 mmol), PyBM (0.600 g, 3 mmol), sodium hydroxide (0.12 g, 3 mmol) and DMF (30 ml) was stirred and heated in N_2 at 120 °C for 12 h. The solution was subsequently poured into ice water (100 ml), after extraction with dichloromethane (3 × 30 ml). The organic layer was extracted one more time with water and dried over anhydrous Mg_2SO_4. The solvent was then evaporated, the resulting residue was purified by silica gel column chromatography to give 0.11 g product (yield, 16%). ^1H NMR (500 MHz, $CDCl_3$): δ 5.89 (s, 6H), 6.90 (s, 3H), 7.05–7.08 (t, 3H), 7.14–7.19 (t, 6H), 7.28–7.32 (d, 3H), 7.69–7.73 (t, 3H), 7.83–7.85 (d, 3H), 8.19–8.26 (d, 6H). EI-MS: m/z: 700 (M^+).

A solution of DBM (0.20 g, 0.9 mmol) and TMMB (75 mg, 0.1 mmol) was dissolved in a mixture of hot ethanol/chloroform with stirring. The solution turned yellow immediately after addition of sodium hydroxide (36 mg, 0.9 mmol). $EuCl_3{\cdot}(H_2O)_6$ (36.6 mg, 0.1 mmol) solved in 2 ml ethanol was added dropwise to the solution. The mixture was continued stirring at 60 °C for 1 h. The products (with red color) were collected by filtration and recrystallized with ethanol. About 75% products were recovered after above purification procedure. Elemental analysis for $C_{180}H_{132}N_9O_{18}Eu_3$. Calcd: C, 68.11; H, 4.69; N, 4.20. Found: C, 68.31; H, 4.16; N, 3.97. Fourier-transform IR spectroscopy (KBr pellet): [cm^{-1}] 3058, 3025, 2966, 2928, 1549, 1518, 1458 (C═O, chelated to Eu^{3+}), 618, 508, 413 (O—Eu—O), 3425 (N—H), 1595 (C═N), 1550, 1478 (imidazolering).

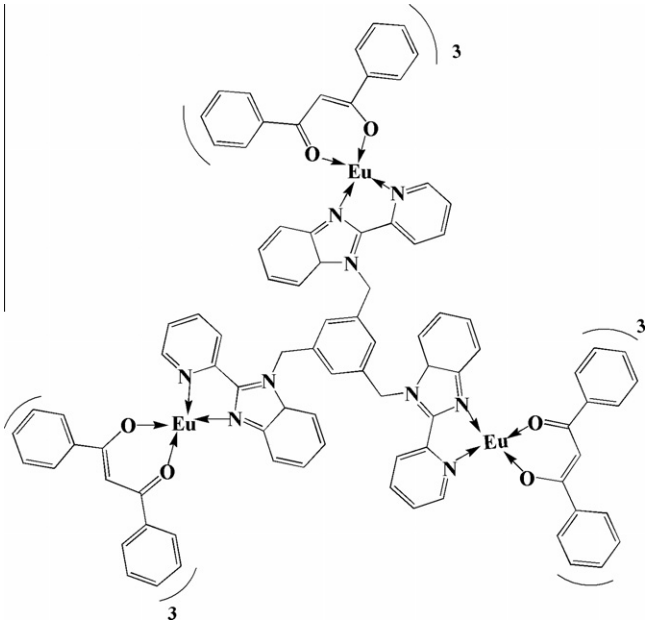

Fig. 1. The chemical structure of $Eu_3(DBM)_9(TMMB)$.

2.2. Fabrication and characterization of the organic electroluminescent device

The other materials, including N,N-bis(naphthylphenyl)-4,4′-biphenyldiamine (NPB), bathocuproine (BCP), 4,4′-bis(carbazole-9-yl)-biphenyl (CBP), and tri(8-hydroxyquinoline)aluminum (Alq_3), were commercially available and applied without further purification.

A pre-patterned indium tin oxide (ITO) coated glass substrate with a sheet resistance of 30 Ω/□ was cleaned by acetone, glass detergent sonication and rinsed with deionized water. After UV ozone treatment, the ITO substrates were loaded in a vacuum chamber. All the organic layers, LiF and Al cathode were sequentially neatly deposited onto the ITO substrates by thermal evaporation at a pressure of 2×10^{-4} Pa. The thickness of depositing film of above materials was monitored by a quartz oscillators and controlled at a rate of 0.2–0.4 nm/s for the organic layers and LiF, and 1.0 nm/s for the Al layer, respectively. The active area of typical device was 10 mm^2. Absorption and PL emission spectra of $Eu_3(DBM)_9(TMMB)$ were measured with a Cary 500 Scan UV–Vis–NIR Spectrophotometer and Cany Eclipse Spectrophotometer, respectively. Electrochemical measurements were performed on a CHI830b electrochemical workstation (CH Instruments, Shanghai Chenhua Instrument Corporation, China) in a conventional three-electrode cell with a platinum-sheet working electrode, a platinum-wire counter electrode, and a silver/silver nitrate (Ag/Ag^+) reference electrode. All electrochemical experiments were carried out under a nitrogen atmosphere at room temperature. The measurements on the EL spectra, Commission International de l'Eclairage (CIE) coordinates and the brightness-current–voltage (*B-I–V*) characteristics were carried out with a Spectrascan PR650 photometer and a computer-controlled direct current power supply. All measurements were carried out in ambient air at room temperature without being especially pointed out.

3. Results and discussion

The structure of $Eu_3(DBM)_9(TMMB)$ contains three Eu(III) cores as branching centers, combining three DBM ligands and one phlydentate ligand of TMMB serving as the connector along the branches of a dendritic structure, as shown in Fig. 1. Excellent optical properties of $Eu_3(DBM)_9(TMMB)$ are expected because of its large rigid structure of complex supported by the central TMMB ligand and high absorption efficiency coming from antenna ligand of DBM.

3.1. Optical properties

The absorption spectra of $Eu_3(DBM)_9(TMMB)$, HDBM and TMMB were measured in solid state and shown in Fig. 2. The absorption spectrum of $Eu_3(DBM)_9(TMMB)$ consists of three main absorption peaks at 318, 333 and 345 nm, respectively. TMMB contributes to the absorption at 318 nm. The other two intense absorption bands locate at 333 and 345 nm match the absorption spectrum of HDBM associated with the π–π^* transition of DBM ligand. Therefore, DBM serves as a strongly-absorbing "antenna" for light harvesting in the complex. The singlet state energy level of TMMB is calculated to be 3.54 eV (350 nm) from its absorption edge.

The phosphorescence spectrum of complex $Gd(TMMB)(NO_3)_3$ measured under 77 K is shown in Fig. 3. From the phosphorescence

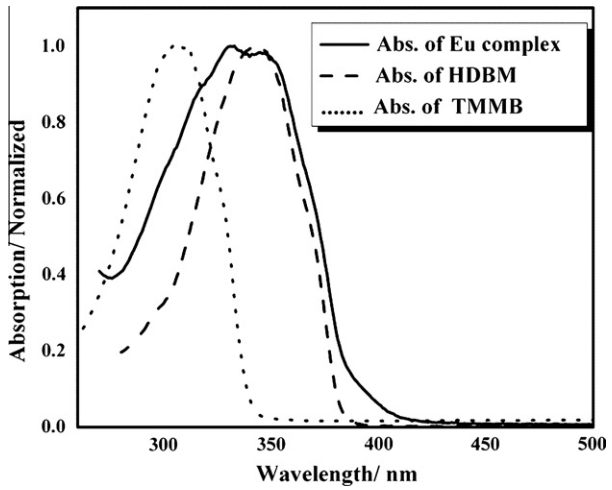

Fig. 2. Absorption spectra of $Eu_3(DBM)_9(TMMB)$, HDBM and TMMB in solid state.

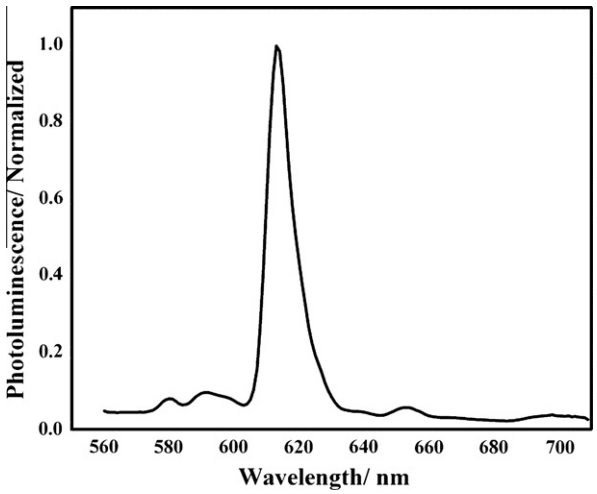

Fig. 4. Phtotoluminescence spectra of complex $Eu_3(DBM)_9(TMMB)$.

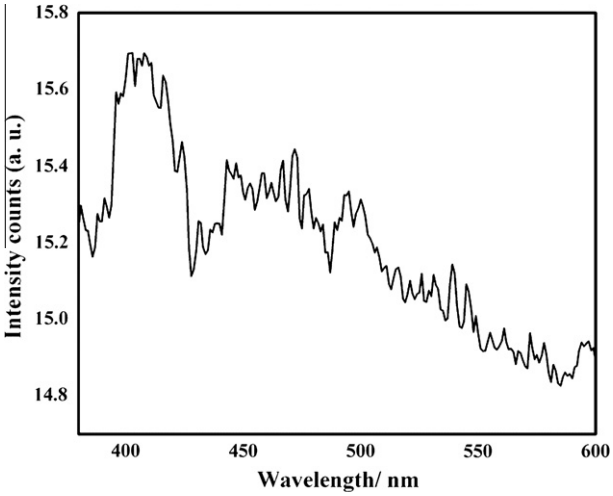

Fig. 3. Phosphorus spectrum of complex $Gd(TMMB)(NO_3)_3$.

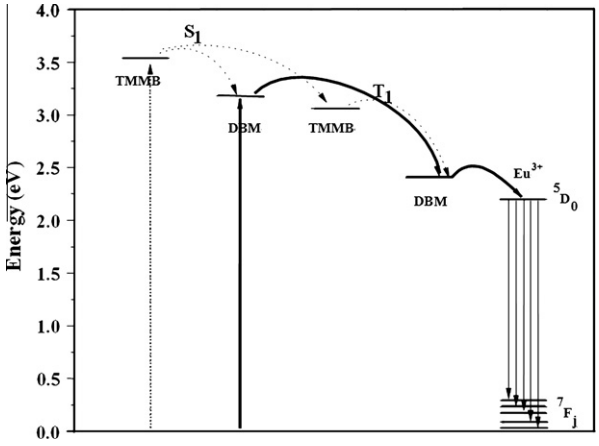

Fig. 5. Schematic energy level diagram and the energy transfer process.

spectrum, the triplet energy level, which correlates with its peak emission wavelength, is calculated to be 3.06 eV (405 nm).

The sharp characteristic emission at 613 nm of the $^5D_0 \rightarrow {}^7F_2$ transition of Eu(III) ion is observed and accompanied by weak emissions of 580, 599, 653 and 698 nm corresponding to $^5D_0 \rightarrow {}^7F_J$ ($J = 0,1,3,4$) upon excitation of 340 nm, as shown in Fig. 4.

This phenomenon can be explained by the energy transfer between ligands and the central metal ion as follows. The singlet state energy levels of DBM and TMMB are estimated by referencing their absorbance edges, which are calculated to be 3.18 eV (390 nm) and 3.54 eV (350 nm). The schematic energy level diagram and energy transfer process are estimated and depicted in Fig. 5. Based on the absorption spectra, we conclude that the majority of excited energy is harvested by DBM, serving as the energy absorbing antenna in the whole complex and also as the starting point of the intramolecular energy transfer process. The energy gap between S_1 and T_1 of DBM is 0.78 eV, which is appropriate for efficient energy transfer. The energy transfer process may consist of two possible pathways: (i) the dominating intramolecular energy transfer process can be described as follows: firstly DBM is excited to its S_1 state, then the energy transfers to its T_1 level and finally to $^5D_0$ level of Eu^{3+}. (ii) A minor part of energy is absorbed by TMMB, and the energy transfers to its T_1 level or S_1 level of DBM. Consequently, all of the energy converges on T1 level of DBM and finally transfers to $^5D_0$ level of Eu^{3+}. Dendritic structure with three DBM ligands as "absorption antennas" facilitates the energy absorption and transportation of the complex.

3.2. Electrochemical properties

The electrochemical property of $Eu_3(DBM)_9(TMMB)$ is investigated by cyclic voltammerty (CV) at room temperature in acetonitrile against an Ag/Ag^+ (0.1 M in acetonitrile) electrode. $Eu_3(DBM)_9(TMMB)$ displays one irreversible oxidation peak with onset potential of 1.18 V and one reduction wave with onset potential of −1.32 V. According to following equations reported by De Leeuw et al. [16]:

$$E_{HOMO} = -(E^{Oxid}_{onset \rightarrow SCE} + 4.4)\text{eV}$$
$$E_{LUMO} = -(E^{Red}_{onset \rightarrow SCE} + 4.4)\text{eV}$$

The E_{HOMO} and E_{LUMO} values of $Eu_3(DBM)_9(TMMB)$ are calculated to be −5.58 eV and −3.08 eV, respectively. The complex with such a narrow energy gap of 2.5 eV is suitable to be used as a guest in host–guest light-emitting diodes. In order to reduce fluorescence quenching effect, CBP, owing a higher LUMO level of −2.7 eV and a lower HOMO level of −6.0 eV, is introduced as host material.

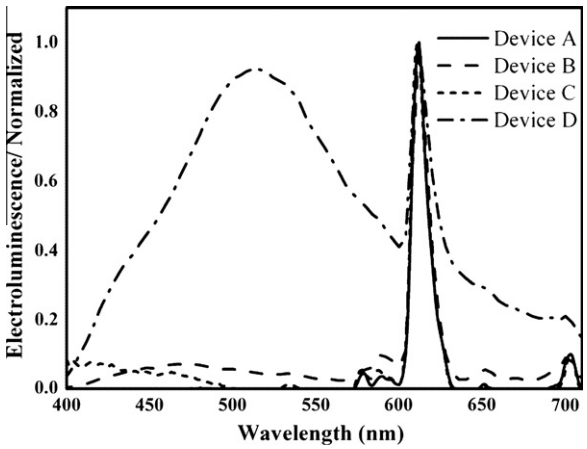

Fig. 6. EL spectra of the four devices upon driving voltage of 14 V.

3.3. EL performances

In order to investigate fluorescence quenching effect and the electron transporting property of $Eu_3(DBM)_9(TMMB)$, four devices (A–D) were designed and fabricated for comparison.

Device A: ITO/NPB (30 nm)/$Eu_3(DBM)_9(TMMB)$ (60 nm)/LiF (1 nm)/Al(100 nm);
Device B: ITO/NPB (30 nm)/$Eu_3(DBM)_9(TMMB)$ (40 nm)/BCP (30 nm)/LiF (1 nm)/Al(100 nm);
Device C: ITO/NPB(30 nm)/CBP:1%$Eu_3(DBM)_9(TMMB)$(40 nm)/BCP(30 nm)/LiF(1 nm)/Al(100 nm);
Device D: ITO/NPB (30 nm)/$Eu_3(DBM)_9(TMMB)$ (40 nm)/Alq_3 (30 nm)/LiF (1 nm)/Al(100 nm).

EL spectra of the four devices are shown in Fig. 6. Among them, EL spectra of devices A–C are red emissions and consistent with the PL spectra of $Eu_3(DBM)_9(TMMB)$. Device D shows near-white emission with two peaks of 525 and 613 nm. EL performances of the four devices are shown and summarized in Fig. 7 and Table 1. We can conclude from Table 1 that device D has the best performance among the devices.

In device A, $Eu_3(DBM)_9(TMMB)$ is used as both emitting and electron transporting layer, while in device B, BCP was inserted as carrier-transporting layer in order to improve the electron injection and transporting property. We found that the turn-on voltage of device B is much lower than that of device A, and the maximum brightness of device B is twice as much as that of device A, which are caused by the lower LUMO level and better carrier-transporting property of BCP. The energy barrier (0.8 eV) between BCP and Al is lower than the gap (1.2 eV) between $Eu_3(DBM)_9(TMMB)$ and Al, so the electron injection is much easier from Al to BCP than that from Al to $Eu_3(DBM)_9(TMMB)$ (Fig. 8). At the same time, BCP may also serves as a hole blocking layer in device B because of its low HOMO energy level, further improving the EL performance of device B.

Device C introduces a doping structure of CBP: $Eu_3(DBM)_9$-(TMMB), reducing the concentration quenching effect. We found that the performance of device C is affected by the doping concentration of $Eu_3(DBM)_9(TMMB)$ in CBP. When the doping concentration is given as 0.5%, 1.0%, 1.5% and 2%, the main luminescent peak at 613 nm in EL spectrum is maintained, while the maximum brightness are 87, 109, 98 and 70 cd m^{-2}, corresponding turn-on voltage are 5, 5, 7 and 8 V respectively. It indicates that the brightness and the efficiency are reduced and the turn-on voltage is raised when the doping concentration is higher than 1%. So we choose 1% as an example to measure the performance of device C. The maximum brightness and maximum current efficiency increase to 109 cd m^{-2} and 0.70 cd A^{-1}, respectively, with the turn-on voltage as low as 5 V. The improved EL performance of device C demonstrates that the energy transfer in host–guest system is effective. Meanwhile, CBP acts as the electron blocking material to prevent electron transferring into NPB layer and combining with

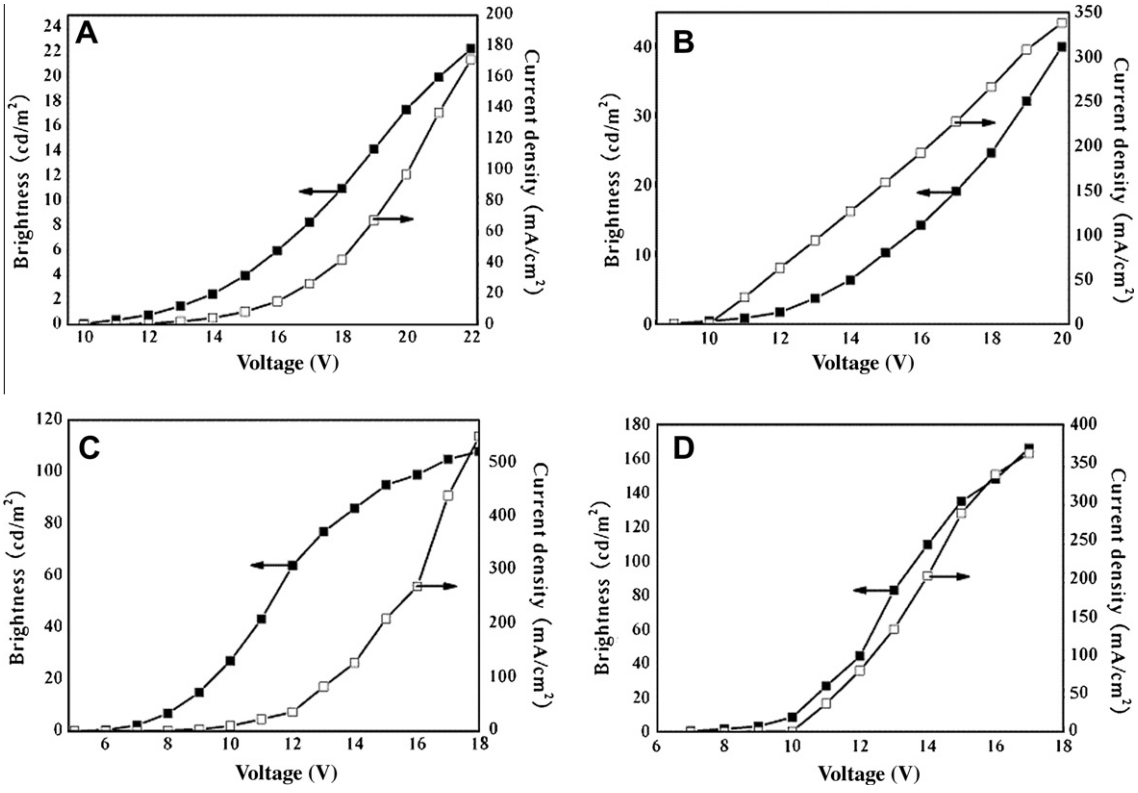

Fig. 7. Brightness-current density–voltage (*B–I–V*) curves of the four devices.

Table 1
EL properties of the devices.

Device	Turn-on voltage (V)	Brightness (cd m^{-2})/ voltage (V)	Current efficiency (cd A^{-1})	CIE (x,y)/15 V
A	10	22/22	0.08	0.67, 0.35
B	9	40/20	0.05	0.60, 0.34
C	5	109/19	0.70	0.64, 0.33
D	7	166/17	0.93	0.31, 0.39

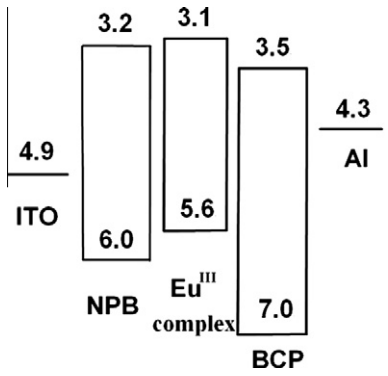

Fig. 8. Energy level schemes of device B.

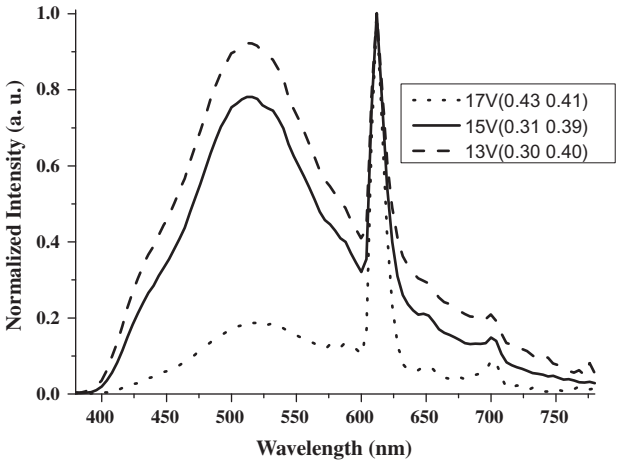

Fig. 9. EL spectrum of device D at different driving voltages (normalized to the Eu^{3+} peak at 613 nm).

the hole in NPB. Such blocking effect eliminates the NPB emission. Correspondingly, pure red emission is acquired in device C.

The EL spectrum of device D gives a white emission with one broad peaking at 460 nm emitted by NPB, 520 nm by Alq_3 and one sharp peak at 613 nm by $Eu_3(DBM)_9(TMMB)$. White emission comes from the simultaneous emission of NPB, Alq_3 and $Eu_3(DBM)_9(TMMB)$, indicating that the combination area locates at the NPB/$Eu_3(DBM)_9(TMMB)$ and $Eu_3(DBM)_9(TMMB)/Alq_3$ interfaces. The emission spectrum overlaps the whole visible region from 400 to 700 nm. Some works have been reported to address the color change issue by independently bias different color OLEDs in a stack structure [17]. In this work, the light spectrum of device D at different bias is shown in Fig. 9. The CIE coordinates are changed at 13 V (0.30, 0.40), 15 V (0.31, 0.39) and 17 V (0.43, 0.41). It is due to the fact that the recombination area moved from the interface between Alq_3 and $Eu_3(DBM)_9(TMMB)$ to $Eu_3(DBM)_9$ (TMMB) layer. At lower bias, the recombination of the hole and electron is located in the interface between Alq_3 and $Eu_3(DBM)_9$ (TMMB) layer. We obtain almost equivalent emission of Alq_3 and $Eu_3(DBM)_9(TMMB)$ at 15 V, and the CIE (0.31, 0.39) is proximate to white emission among the CIE under different biases. At the higher driving voltage of 17 V, carrier recombination area mainly located in $Eu_3(DBM)_9(TMMB)$ layer, so strong emission of $Eu_3(DBM)_9(TMMB)$ and weak Alq_3 emission are achieved. The simultaneous emission of $Eu_3(DBM)_9(TMMB)$ and Alq_3 causes the markedly increasing of efficiency. As shown in Fig. 4 (D). A maximum luminance of 166 cd m^{-2} is achieved at the driving voltage of 17 V. A maximum current efficiency is 0.93 cd A^{-1}. This is a representative sample of simple white device structure to obtain blue, green and red emission simultaneously. If $Eu_3(DBM)_9$ (TMMB):Alq_3 doped structure is used, the light emitting efficiency may be further improved.

4. Conclusion

Four EL devices (A–D) with red and white emission have been fabricated. Characteristic red emission peak of 613 nm due to the $^5D_0 \rightarrow {}^7F_2$ transition of Eu(III) ion is observed for devices A–C. Moreover, the host–guest doping structure (device C) obtains higher maximum luminance (109 cd m^{-2}) and maximum current efficiency (0.70 cd A^{-1}) than device A and B owing to the decrease of the concentration quenching effect and the increase of the carrier injection and transportation by inserting BCP layer. Device D shows broad band white emission of CIE (0.31, 0.39), which overlaps visible spectrum from 400 to 700 nm, with simple non-doping device structures. The maximum luminance and maximum current efficiency are 166 cd m^{-2} and 0.93 cd A^{-1}, respectively. The simplified device structure without doping makes the fabrication of organic white light-emitting diodes more convenient and practicable.

Acknowledgements

The authors gratefully acknowledge financial support from NSFC (20971020 and 20903020), 973 Program (2009CB623605), the Science and Technology Development Planning of Jilin Province (201101008, 20100540), and the Training Fund of NENU's Scientific Innovation Project (NENU-STC08012).

References

[1] Kido J, Okamoto Y. Chem Rev 2002;102:2357–67.
[2] Zhu XH, Wang LH, Ru J, Huang W, Fang JF, Ma DG. J Mater Chem 2004;14:2732.
[3] Liang CJ, Choy WCH. Appl Phys Lett 2006;89:251108.
[4] Liang CJ, Choy WCH, Huang CH. IEEE Photon Technol Lett 2007;19:1178–80.
[5] Holder E, Langevekd BMW, Schubert US. Adv Mater 2005;17:1109–21.
[6] Burn PL, Lo SC, Samuel IDW. Adv Mater 2007;19:1675–88.
[7] Hwang SH, Moorefield CN, Newkome GR. Chem Soc Rev 2008;37:2543–57.
[8] Hwang SH, Shreiner CD, Moorefield CN, Newkome GR. New J Chem 2007;31:1192–217.
[9] Lo SC, Burn PL. Chem Rev 2007;107:1097–116.
[10] Li SF, Zhong G, Zhu WH, Li FY, Pan JF, Huang W, et al. J Mater Chem 2005;15:3221–8.
[11] Chen CH, Lin JT, Yeh MCP. Org Lett 2006;8:2233–6.
[12] Wang BB, Fang JF, Li B, You H, Ma DG, Hong ZR, et al. Thin Solid Films 2008;516:3123–7.
[13] Xu H, Yin K, Huang W. ChemPhysChem 2008;9:1752–60.
[14] Xu H, Yin K, Huang W. Synth Met 2010;160:2197–202.
[15] Balzani V, Bergaminni G, Ceroni P, Vogtle F. Coord Chem Rev 2007;251:525–35.
[16] De Leeuw DM, Simenon MMJ, Brown AR, Einerhand REF. Synth Met 1997;87:53–9.
[17] Liang CJ, Choy WCH. J Organomet Chem 2009;694:2712–6.